Check for updates

Original Research Article

Chrysoeriol Inhibits Viability and Triggers Caspase-dependent Apoptosis in Thyroid Cancer TPC-1 Cells

Pharmacognosy Magazine
22(4) 1481–1496, 2026
© The Author(s) 2026
Article reuse guidelines:
in.sagepub.com/journals-permissions-india
DOI: 10.1177/09731296261444852
journals.sagepub.com/home/phm
Sage

Xi Dong[1], Xiaodong Li[1], Shuheng Li[1], Weiying Ge[2] and Na Feng[2]

Abstract

Background: Thyroid cancer represents the most prevalent endocrine cancer, with papillary thyroid carcinoma responsible for the most cases and presenting a significant clinical challenge due to its variable prognosis.
Objectives: This work aims to examine the effects of chrysoeriol on thyroid cancer TPC-1 cells, by targeting apoptotic mediators caspase-3, caspase-8, and caspase-9 through molecular docking and evaluating their expression in TPC-1 cells treated with chrysoeriol under *in vitro* conditions.
Materials and Methods: The cytotoxic effects of chrysoeriol on the growth of thyroid cancer TPC-1 cells were assessed using an MTT assay. The extent of apoptosis in both untreated and chrysoeriol-treated TPC-1 cells was examined using a dual staining approach. The activity of caspase enzymes (caspase-3, caspase-8, and caspase-9) in untreated and chrysoeriol-exposed TPC-1 cells was assessed using commercial test kits. In addition, the potential interactions of chrysoeriol and doxorubicin (DOX) with the caspase-3, caspase-8, and caspase-9 were evaluated by implementing molecular docking studies.
Results: The treatment of diverse dosages of chrysoeriol effectively inhibited thyroid cancer TPC-1 cells in a dose-dependent manner. Moreover, chrysoeriol treatment markedly increased apoptosis in TPC-1 cells, as demonstrated by the results of the dual staining method. Furthermore, treatment with chrysoeriol also increased the activity of caspase-3, caspase-8, and caspase-9 in thyroid cancer TPC-1 cells. Molecular docking predicted a better interaction of caspase-3 (binding affinity (BA) = −6.7 kcal/mol; RMSD = 1.307Å), caspase-8 (BA = −6.5 kcal/mol; RMSD = 1.709Å), caspase-9 (BA = −6.6 kcal/mol; RMSD = 2.08Å) with the chrysoeriol and caspase-3 (BA = −6.3 kcal/mol; RMSD = 2.757Å), caspase-8 (BA = −6.3 kcal/mol; RMSD = 2.398Å), caspase-9 (BA = −6.7 kcal/mol; RMSD = 2.685Å) with the DOX. These computational results suggest that chrysoeriol may interact well with caspase proteins and contribute to their activation as part of its pro-apoptotic mechanism and caspase activation in thyroid cancer TPC-1 cells.
Conclusion: The present study demonstrates that chrysoeriol exhibits anti-cancer properties against thyroid cancer, inhibiting cell growth and inducing apoptosis in TPC-1 cells by upregulating caspase activity. The increased activities of caspase-3, caspase-8, and caspase-9 indicate that chrysoeriol activates both intrinsic and extrinsic apoptotic pathways. Molecular docking and toxicity analysis further support these findings by revealing better binding affinities between chrysoeriol and the caspase proteins than DOX, suggesting that these interactions may facilitate caspase activation. Thus, the current results highlight that chrysoeriol is a hopeful anti-cancer agent for future thyroid cancer treatment.

Keywords

Apoptosis, thyroid cancer, caspase-3, TPC-1 cell line, cytotoxicity, molecular docking, toxicity

Received 05 November 2025; **revised** 04 December 2025; **accepted** 02 April 2026

Introduction

Thyroid cancer, a prevalent endocrine malignancy, develops from the thyroid gland, an essential organ for human metabolism located in the neck. This type of cancer is characterized by the uncontrolled growth of cells within the thyroid, which can manifest in various histological subtypes, including

[1]Department of Nuclear Medicine, Affiliated Hospital of Hebei University, Baoding, Hebei, China
[2]Department of Radiology, Affiliated Hospital of Hebei University, Baoding, Hebei, China

Corresponding author:
Na Feng, Department of Radiology, Affiliated Hospital of Hebei University, Baoding, Hebei 071000, China.
E-mail: na000333@sina.com

Creative Commons Non Commercial CC BY-NC: This article is distributed under the terms of the Creative Commons Attribution-NonCommercial 4.0 License (http://www.creativecommons.org/licenses/by-nc/4.0/) which permits non-Commercial use, reproduction and distribution of the work without further permission provided the original work is attributed as specified on the SAGE and Open Access pages (https://us.sagepub.com/en-us/nam/open-access-at-sage).

papillary, follicular, medullary, and anaplastic carcinomas, each with distinct clinical behaviors and prognoses (Christofer Juhlin et al., 2023). The vast majority, approximately 90%, comprise papillary and follicular thyroid cancers, which are differentiated thyroid carcinomas from follicular epithelial cells. Papillary thyroid cancer accounts for over 80% of all thyroid cancers and typically grows slowly, often spreading initially to local lymph nodes (Pizzato et al., 2022). In contrast, medullary thyroid cancer develops from parafollicular C-cells, while anaplastic thyroid cancer is an aggressive, undifferentiated form originating from follicular cells. Poorly differentiated and anaplastic thyroid cancers, though less common, present significant challenges due to their aggressive nature and reduced responsiveness to standard therapies. While often asymptomatic, thyroid nodules, which are distinct lesions stemming from abnormal localized growth of thyroid cells, are the most common thyroid pathology, with nearly 5% of these nodules proving to be malignant (Kitahara & Schneider, 2022). Despite this, the majority of thyroid malignant neoplasms are categorized as low-risk, exhibiting low recurrence rates and favorable survival outcomes. However, even among well-differentiated types, recurrence and mortality rates can be higher in specific patient cohorts, warranting careful stratification and tailored management (Lamartina et al., 2021).

Despite a generally favorable prognosis with treatment, advanced cases, particularly among young women, frequently experience recurrence, leading to a diminished 10-year disease-specific survival rate. Therefore, a deeper mechanistic understanding of thyroid cancer progression is critical for developing novel therapeutic interventions and enhancing patient outcomes (Siegel et al., 2023). One such crucial mechanism is apoptosis, a tightly regulated mechanism of programmed cell death crucial for cellular homeostasis, and its dysregulation is increasingly recognized as a hallmark of cancer. Aberrant apoptosis pathways contribute to both tumor initiation and progression in various malignancies, including thyroid cancer. The dysregulation of apoptotic pathways often underpins tumor proliferation and aggressiveness, rendering them critical targets for the development of anti-cancer treatments in thyroid malignancies (Zhao et al., 2025).

Current conventional treatments for thyroid cancer typically involve surgical intervention, radioactive iodine therapy, and thyroid-stimulating hormone suppressive therapy, which can be used individually or in combination. However, despite the generally favorable prognosis for well-differentiated thyroid cancers, a significant subset of patients (approximately 10%) exhibit resistance to radioactive iodine therapy and face a higher probability of recurrence (Dierks et al., 2021; Thumpati et al., 2025). For these advanced cases, particularly poorly differentiated or undifferentiated thyroid cancers, treatment options remain limited and present substantial therapeutic challenges. Approximately 5% of all thyroid cancer patients develop metastasis that fails to respond to radioactive iodine, further highlighting the urgent need for novel therapeutic strategies (French et al., 2024).

While surgery and radioactive iodine effectively manage differentiated thyroid cancer, concerns regarding systemic exposure to radiation and the potential for secondary malignancies highlight the need for improved approaches. These challenges underscore the critical need for developing safer and more effective alternative therapies, particularly for advanced or refractory forms of thyroid cancer (Busaidy et al., 2022). Therefore, ongoing research is increasingly focusing on innovative therapeutic modalities that can circumvent these limitations and deliver improved patient outcomes. Therefore, there is a mounting interest in exploring natural compounds, particularly those derived from plants, as potential sources for novel anti-cancer agents with improved efficacy and reduced toxicity (Kaczmarzyk et al., 2024). Chrysoeriol, a 3′-*O*-methoxy flavone polyphenol, is a bioactive flavonoid compound found in numerous tropical medicinal plants, including *Coronopus didymus, Eurya cilliata, Eremosparton songoricum, Medicago sativa*, and *snapdragons* (*Antirrhinum majus*). The various biological activities of chrysoeriol have already been reported previously, including its anti-inflammatory (Wu et al., 2020), antioxidant (Kim et al., 2021), nephroprotective (Qiu & Xu, 2021), and cardioprotective (Liu et al., 2009) properties. Furthermore, chrysoeriol has already shown anti-cancer activities against various cancer cells, including lung cancer (Wei et al., 2019), glioma (Wongkularb et al., 2022), pancreatic cancer (Zhang et al., 2018), melanoma (Liu et al., 2023), and breast cancer (Min et al., 2020) cells. In addition to its pharmacological effects, the anti-cancer potential of chrysoeriol against thyroid cancer has yet to be evaluated. Hence, this study aims to examine the effects of chrysoeriol on thyroid cancer TPC-1 cells, by targeting caspase activation through *in vitro* and *in silico*, which offers novel insights into the anti-thyroid cancer mechanisms of chrysoeriol.

Materials and Methods

Chemicals

Chrysoeriol, Dulbecco's Modified Eagle Medium (DMEM), dimethyl sulfoxide (DMSO), antibiotics, and other chemicals were procured commercially from Sigma–Aldrich, USA. The test kits for quantifying caspase activities were obtained from Elabscience, USA.

Maintenance of Cell Culture

Thyroid cancer TPC-1 cells were purchased commercially from ATCC, USA, and cultivated in DMEM enriched with 10% FBS and 1% anti-mycotic cocktail in a 5% CO_2 incubator. The mature cells were collected upon achieving 80% confluency and were subjected to further experiments and biochemical assays.

MTT Cytotoxic Assay

The growth of untreated and chrysoeriol-treated TPC-1 cells was investigated using the MTT assay. Cells were loaded on a 96-well plate at 5×10^3 cell density/well and subsequently treated with chrysoeriol at diverse dosages (5, 10, 15, 20, 25, and 30 μM) for a duration of 24 h. Following the treatment, MTT (20 μL) solution was added with DMEM (100 μL) in the wells for a duration of 4 h. After dissolving the generated formazan deposits with DMSO (100 μL), the absorbance of the culture plate was measured at 570 nm.

Analysis of Apoptotic Cell Death by the Dual Staining Method

The dual staining assay was conducted on the untreated and chrysoeriol-treated TPC-1 cells to evaluate their apoptosis levels. The TPC-1 cells were grown in a 24-well plate at 5×10^5 cells/well and subsequently exposed to 20 μM of chrysoeriol and/or 2 μg of doxorubicin (DOX) for an additional 24 h. Subsequently, AO/EB (100 μg/mL) dye was mixed into the wells for 5 min in darkness to evaluate apoptosis in TPC-1 cells using a fluorescence microscope.

Analysis of Caspase Enzyme Activities

TPC-1 cells, both untreated and subjected to chrysoeriol treatment, were collected and lysed with cell lysis buffer to generate cell lysates. The resultant cell lysate was undergoing centrifugation at 5,000 rpm for 15 min, and the supernatant was utilized to evaluate caspase activities. Caspase-3, caspase-8, and caspase-9 activities were analyzed in cell lysates using commercially purchased test kits according to the manufacturer's guidelines (Abcam, USA). The enzyme activity was normalized to the protein content, which was measured using the Bradford method.

In Silico Analysis

The Dataset Retrieval for Molecular Docking Analysis

Targets such as caspase-3, caspase-8, and caspase-9 sequences were retrieved from the AlphaFold database, and the structures were validated using the Ramachandran Plot (RM) by accessing SAVES v6.1 (https://saves.mbi.ucla.edu/) (Varadi et al., 2024). Then, the structures were refined using GalaxyRefine (https://galaxy.seoklab.org/) (Heo et al., 2013) to improve model quality and further validated using an RM plot.

Active Site Prediction and Preparation of Ligand

The active sites were predicted for the improved target models using PrankWeb (https://prankweb.cz/) (Jendele et al., 2019). After, the chrysoeriol and doxorubicin structures were prepared using Discovery Studio Visualizer (DSV) v19.1.0.18287 (www.accelerys.com) to perform molecular docking. In this regard, the chrysoeriol and doxorubicin structures were obtained from the PubChem compound database in SDF format with 3D atomic coordinates provided, and converted into PDB format using DSV.

Molecular Docking and Visualization

The molecular docking process was performed for the targets, caspase-3, caspase-8, and caspase-9 with chrysoeriol and doxorubicin using AutoDock Vina, integrated with PyRx software (Eberhardt et al., 2021). The AutoDock Vina is built with an advanced scoring algorithm. This process predicts the most favorable binding modes between the caspase-3, caspase-8, caspase-9, and the ligand.

The AutoDock Vina uses a new scoring mechanism,

$$C = \sum_{i<j} f_{titij}\left(r_{ij}\right),$$

C: Sum of intermolecular and intramolecular distance; ∑: Over all of the pairs of atoms; f_{titij}: Symmetric set of interaction functions; r_{ij}: Interatomic distance.

The selected targets, namely, caspase-3, caspase-8, and caspase-9, along with the ligands chrysoeriol and doxorubicin, were converted into PDBQT format for molecular docking studies. Docking was performed using the PyRx virtual screening tool after defining the active site residues of each caspase. The grid box dimensions were set as follows: caspase-3 (size_*x, y, z* = 25.24 Å, 25.04 Å, 23.81 Å; center_*x, y, z* = 25.33 Å, 25.44 Å, 22.46 Å), caspase-8 (size_*x, y, z* = 22.54 Å, 25.56 Å, 28.36 Å; center_*x, y, z* = 22.78 Å, 26.12 Å, 29.53 Å), and caspase-9 (size_*x, y, z* = 23.21 Å, 19.41 Å, 16.60 Å; center_*x, y, z* = 22.98 Å, 18.59 Å, 19.47 Å). The docking results were analyzed using DSV to identify the binding interactions of chrysoeriol and doxorubicin with the target caspases. Furthermore, LigPlot+ v2.2.9 (Laskowski & Swindells, 2011) was employed to validate and visualize the hydrogen bonds and hydrophobic interactions within the chrysoeriol- and doxorubicin-caspase complexes.

Toxicity Prediction

The toxicity properties were predicted for the ligands chrysoeriol and DOX by implementing the ProTox v3.0 (https://tox.charite.de/protox3/index.php?site=home) (Banerjee et al., 2024).

Statistical Analysis

The statistical tests were conducted using GraphPad Prism software, and the results are given as a mean ± SD of triplicates. One-way analysis of variance (ANOVA) and Tukey's *post hoc* tests were performed to analyze the data, with $p < .05$ considered significant.

Results

In Vitro

Chrysoeriol Treatment Decreases the Viability of Thyroid Cancer TPC-1 Cells

Figure 1 depicts the findings of the MTT cytotoxicity assay for both untreated and chrysoeriol-treated TPC-1 cells. The treatment with chrysoeriol significantly diminished the growth of TPC-1 cells at doses ranging from 5 to 30 µM, indicating its cytotoxic effects on thyroid cancer cells. The increased dosages of chrysoeriol significantly suppressed the growth of TPC-1 cells. The IC_{50} concentration of chrysoeriol for TPC-1 cells was determined to be 20 µM, and this dosage was selected for additional experiments.

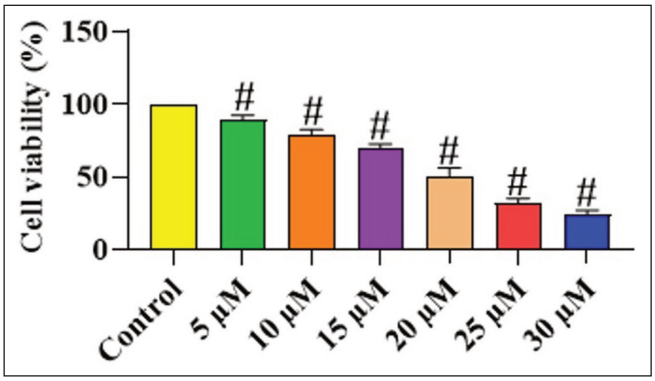


Figure 1. Effect of Chrysoeriol on the Viability of Thyroid Cancer TPC-1 Cells.

Notes: The treatment with chrysoeriol markedly reduced the viability of TPC-1 cells at doses ranging from 5 to 30 µM, demonstrating its cytotoxic effects against thyroid cancer cells. The data were analyzed using GraphPad Prism software, and the outcomes are expressed as a mean ± SD of triplicates. One-way analysis of variance (ANOVA) and Tukey's *post hoc* tests were utilized to evaluate the values. "#" indicates that data were significantly differ from the control group at $p < .05$.

Chrysoeriol Treatment Induces Apoptosis in Thyroid Cancer TPC-1 Cells

The dual staining method was conducted on both untreated and chrysoeriol-treated TPC-1 cells to evaluate their apoptosis levels, and the outcomes are illustrated in Figure 2. The TPC-1 cells demonstrated pronounced red fluorescence after exposure to 20 µM of chrysoeriol, signifying the onset of both early and late apoptotic cell death, respectively. Similarly, the findings of DOX treatment also demonstrated an elevated presence of cells displaying intense red fluorescence, thus demonstrating the onset of apoptosis in TPC-1 cells.

Chrysoeriol Treatment Increases the Activities of Caspase Enzymes in the TPC-1 Cells

The activities of caspase enzymes in the cell lysates from both untreated and chrysoeriol-treated TPC-1 cells were examined, with the findings illustrated in Figure 3. The activities of caspase-3, caspase-8, and caspase-9 were seen to be reduced in the untreated TPC-1 cells. However, the 20 µM of chrysoeriol treatment significantly elevated the activities of caspase enzymes (caspase-3, caspase-8, and caspase-9) in the thyroid cancer TPC-1 cells compared to the control group. These results were further validated by the findings of DOX treatment, which similarly increased the caspase enzyme activities in the TPC-1 cells.

In Silico

The structures of caspase-3, caspase-8, and caspase-9 were obtained from the AlphaFold database, and the quality of the models was validated with the RM plot (caspase-3 = 86.1%; caspase-8 = 88.0%; caspase-9 = 89.1%), which resulted in better models (Figure 4A, 4C, 4E). However, the model required improvement before proceeding into the docking process. Hence, the structures were improved using GalaxyRefine, and the refined models were further validated

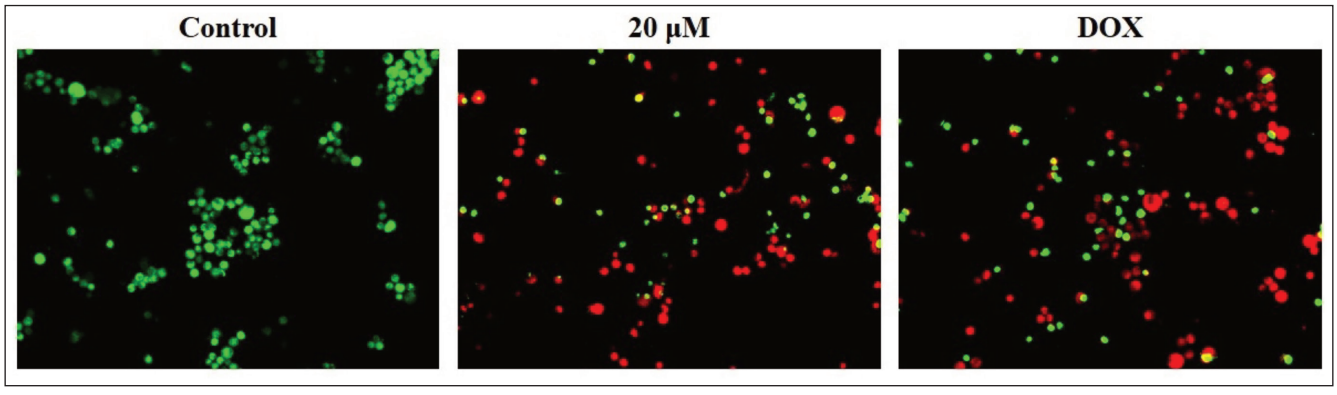


Figure 2. Effect of Chrysoeriol on the Apoptotic Cell Death in Thyroid Cancer TPC-1 Cells.

Note: The thyroid cancer TPC-1 cells had heightened red fluorescence following treatment with chrysoeriol (20 µM) and/or DOX, indicating the occurrence of both early and late stage apoptosis, respectively.

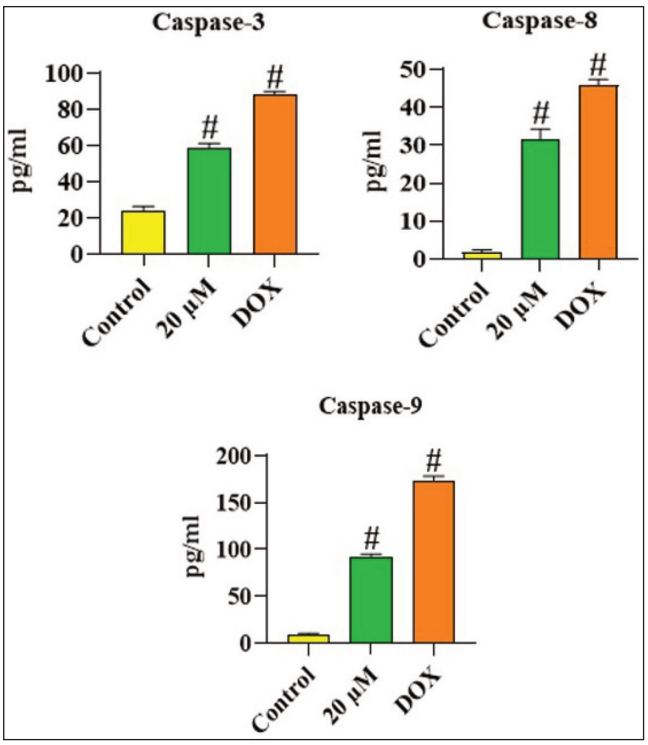


Figure 3. Effect of Chrysoeriol on the Activities of Caspase Enzymes in the TPC-1 Cells.

Notes: The data were analyzed using GraphPad Prism software, and the outcomes are expressed as a mean ± SD of triplicates. One-way analysis of variance (ANOVA) and Tukey's *post hoc* tests were utilized to evaluate the values. "#" indicates that data were significantly differ from the control group at $p < .05$.

with the RM plot (caspase-3 = 95.2%; caspase-8 = 94.5%; caspase-9 = 96.4%) (Figure 4B, 4D, 4F) and implemented for the active site prediction and molecular docking studies with chrysoeriol and DOX. The active sites were predicted for these refined models of caspase-3 (MET61, THR62, SER63, ARG64, SER65, HIS121, CYS163, TYR204, SER205, TRP206, ARG207, SER209, and PHE256), caspase-8 (LEU254, SER256, ILE257, ARG258, ASP259, ARG260, HIS317, GLY318, ASP319, CYS360, GLY362, ASP363, VAL410, SER411, TYR412, and ARG413), and caspase-9 (GLY309, SER310, ASP356, SER359, TRP362, GLU365, LYS394, and GLY395). The resulting binding affinity (BA), RMSD, and the types of bonds involved in the interactions of caspase-3, caspase-8, and caspase-9 with the chrysoeriol and DOX were tabulated in Table 1.

Caspase-3

The chrysoeriol interacted with the residues of caspase-3, which include HIS121, CYS163, SER205, ARG207(2), PHE250CH, and SER251(2), with the BA of −6.7 kcal/mol and the RMSD of 1.307Å. Also, the pi-cation, pi-pi-t-shaped and pi-pi stacked bonds are formed with the residues ARG64(2), TYR204, and PHE256. Also, the hydrophobic residues such as TRP206, PHE252, and ASP253 further stabilize the interactions (Figure 5A, 5B, 5G; Table 1). Likely, the DOX interacted with the residues ARG64, ARG207, PHE252, ASP253, SER205^{CH}, SER251, and formed the hydrogen and carbon hydrogen bonds with the BA of −6.3 kcal/mol and the RMSD of 2.757Å. Meanwhile, the residues such as CYS163, TYR204, and PHE256 interacted with the DOX and formed the pi-alkyl and pi-pi-t-shaped bond, and the residues such as HIS121, ASN208, and SER209 hydrophobically interacted with the DOX and stabilized the complex (Figure 6A, 6B, 6G; Table 1).

Caspase-8

The chrysoeriol interacted with the residues of caspase-8, which include GLY362, ASP363, TYR365, and ARG258, and formed the hydrogen and carbon hydrogen bond with the BA of −6.5 kcal/mol and the RMSD of 1.709Å. The other residues, such as ARG413, ARG260, HIS317, CYS360, and VAL410, interacted with the chrysoeriol via the alkyl, pi-alkyl, and pi-sigma bonds, and the residues, such as ILE257, ASN261, TYR412, and PRO415, hydrophobically interacted with the chrysoeriol (Figure 5C, 5D, 5H; Table 1). Similarly, DOX interacted with the ARG258, TYR365, TYR412, HIS317 and formed the hydrogen bonds with the BA of −6.3 kcal/mol, and the RMSD was observed as 2.398Å. Additionally, the residues ARG258, LEU254, and ASP363 interacted with the DOX and formed the alkyl and pi-anion bonds. Also, the residues such as LYS253, SER256, ILE257, ASP259, ARH413, and ASN458 hydrophobically interacted with the DOX and helped to stabilize the complex (Figure 6C, 6D, 6H; Table 1).

Caspase-9

The caspase-9 residues SER307 and GLY395 interacted with the chrysoeriol via the hydrogen bonds, and the other residue PRO312 formed the pi-alkyl bond with the BA of −6.6 kcal/mol, and the RMSD was observed as 2.08Å. In addition, the residues GLU304, ASP305, GLU306, SER310, ASP356, SER359, GLU365, VAL393, and LYS394 hydrophobically interact with the chrysoeriol and stabilize the complex interactions (Figure 5E, 5F, 5I; Table 1). Similarly, the DOX interacted with the SER310, VAL393, GLY395, LYS394, SER307 residues and formed the hydrogen bonds with the BA of −6.7 kcal/mol and the RMSD of 2.685Å, and the other residues, such as LYS394 and GLU365, formed the pi-alkyl and pi-anion bonds. Meanwhile, the residues such as GLU304, GLU306, GLY309, ASN311, PRO312, ASP356, SER359, ASP369, and ILE396 exhibited the hydrophobic interactions with the DOX and further stabilized the complex (Figure 6E, 6F, 6I; Table 1).

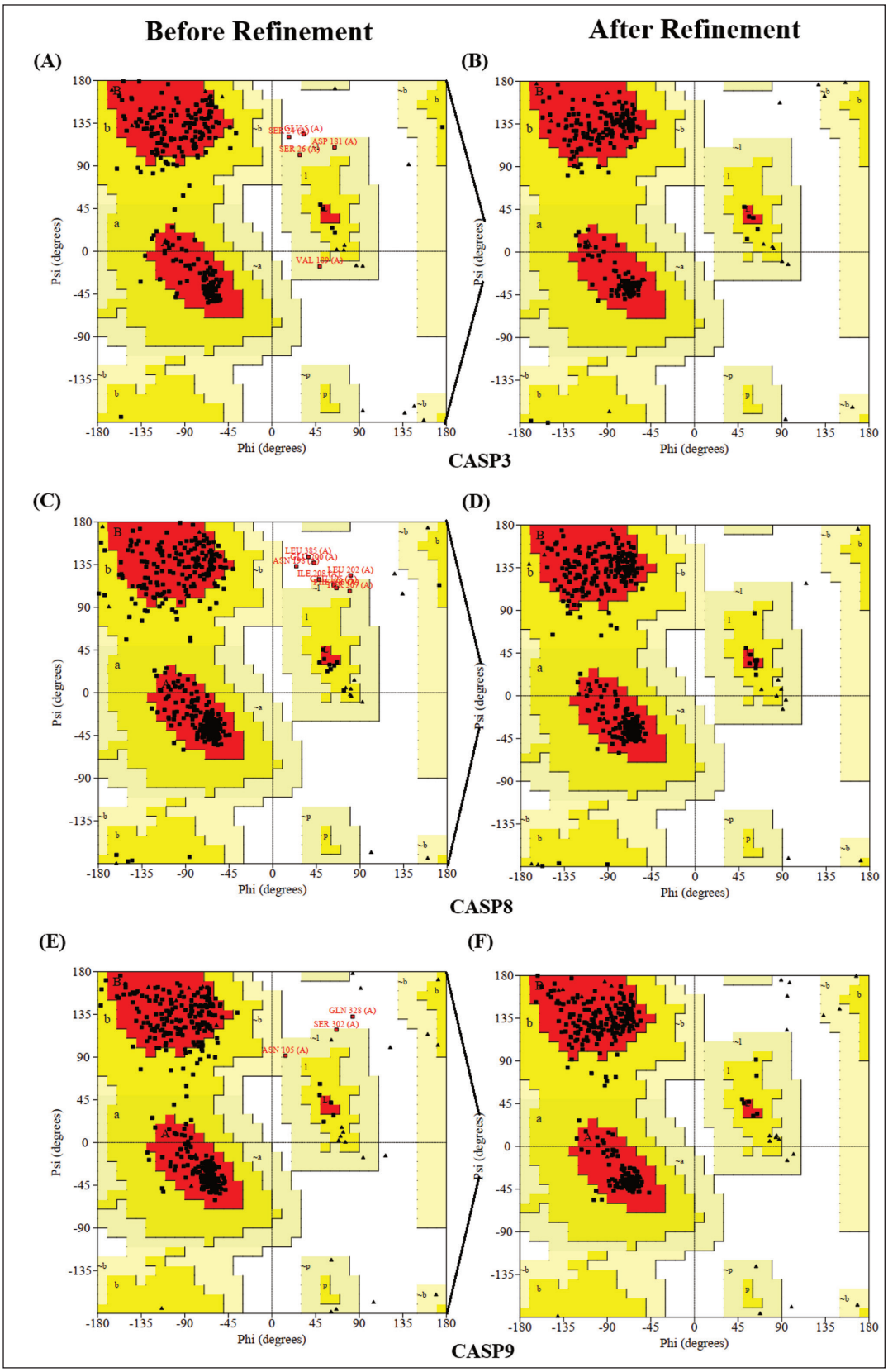


Figure 4. The RM Plot of the Target's Caspase-3, Caspase-8, and Caspase-9 Before and After Refinement.

Notes: (A, C, E) The obtained models of caspase-3, caspase-8, and caspase-9 before refinement (B, D, F) the obtained models of caspase-3, caspase-8, and caspase-9 after refinement.

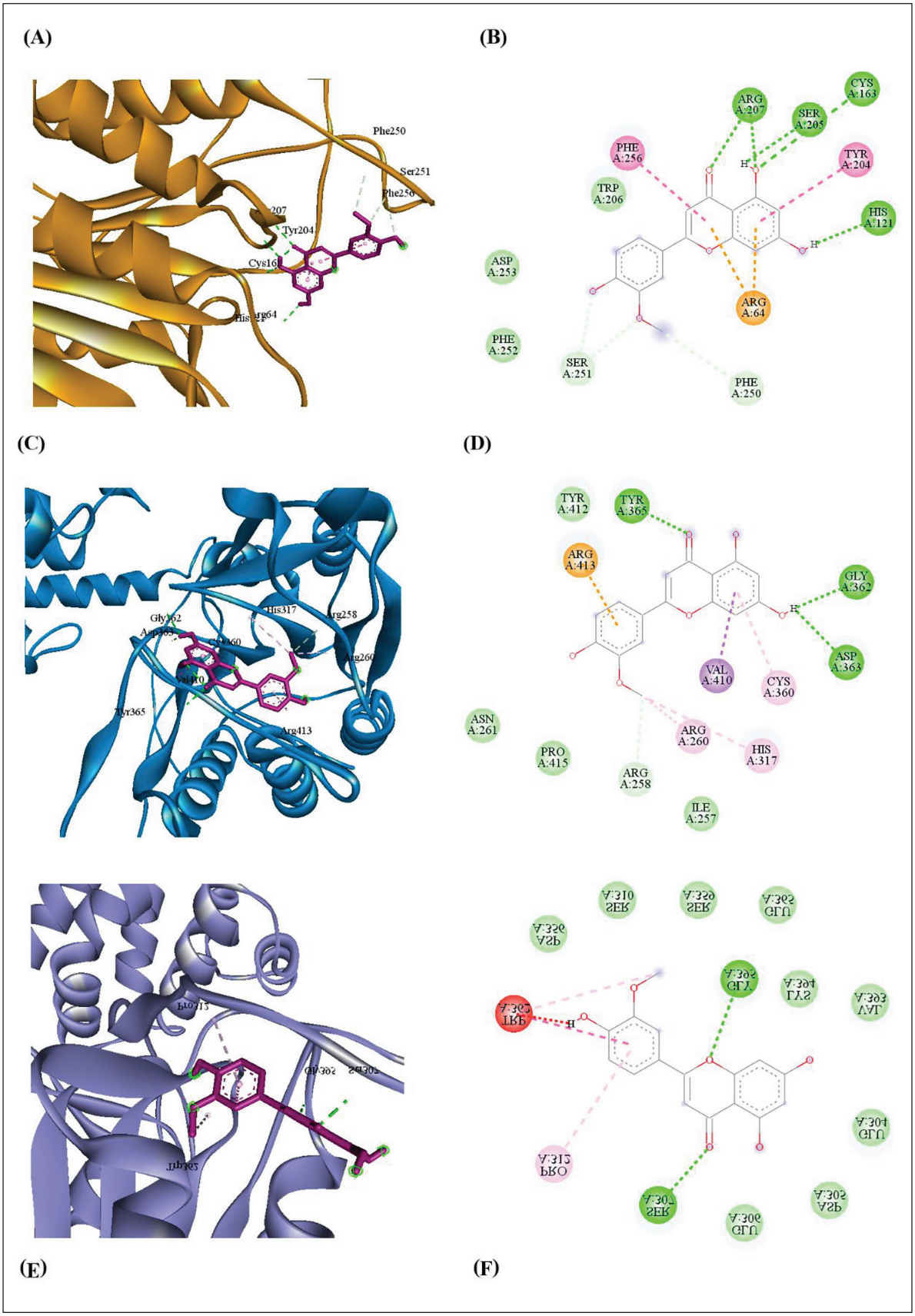


Figure 5. *(continued)*.

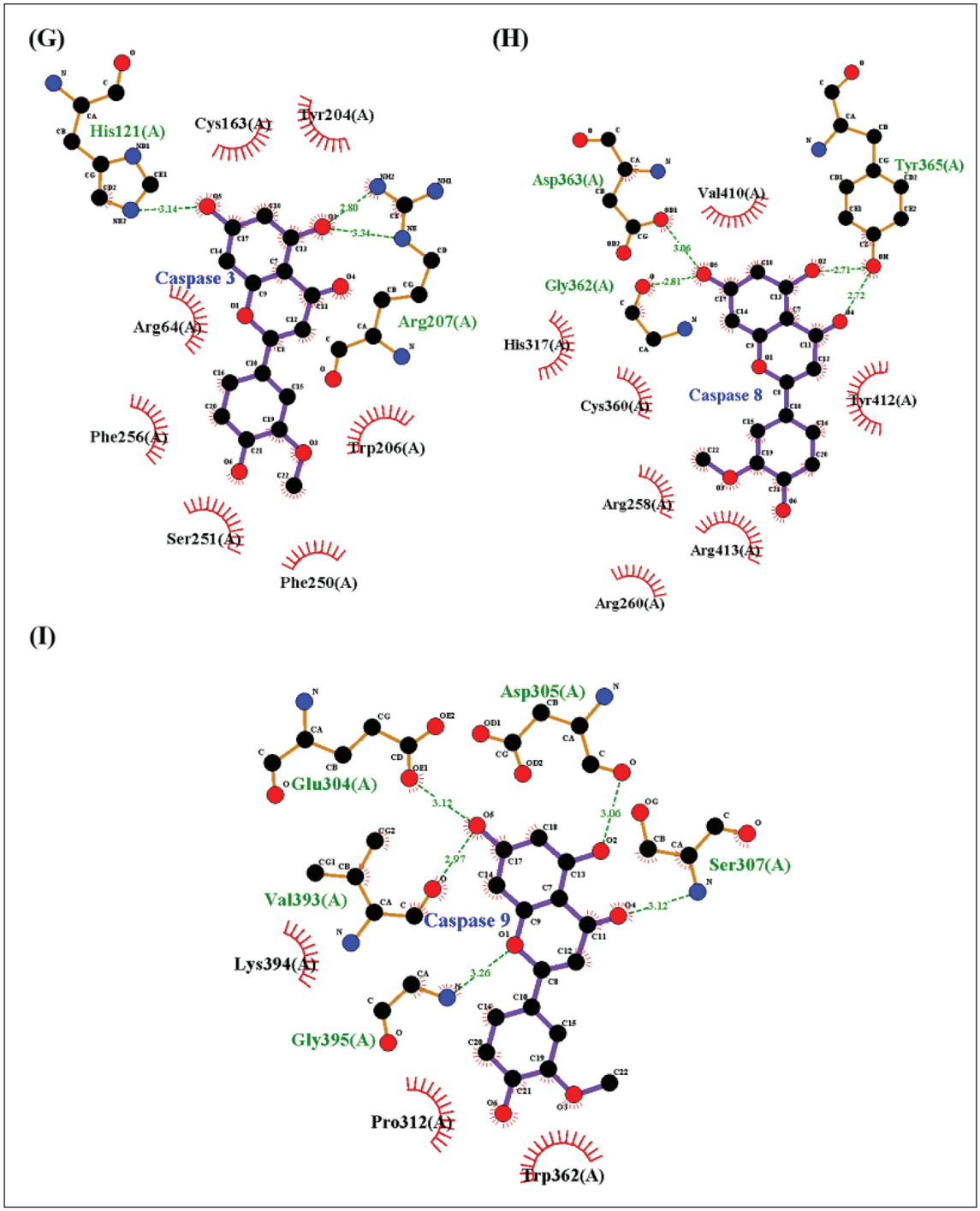


Figure 5. The Three-dimensional (3D) and Two-dimensional (2D) Docking Pose of the Caspase-3, Caspase-8, and Caspase-9 Interacted with the Chrysoeriol and the LigPlot+ Interactions.

Note: (A, B, G) caspase-3 (C, D, H) caspase-8 (E, F, I) caspase-9.

Toxicity Analysis

The toxic properties, such as mutagenicity, immune toxicity, hepatotoxicity, neurotoxicity, respiratory toxicity, nephrotoxicity, cytotoxicity, carcinogenicity, blood–brain–barrier (BBB) effects, lethal dose, and toxicity class, were evaluated for the standard drug DOX and the compound chrysoeriol and tabulated in Table 2. The results stated that chrysoeriol exhibited a comparatively safer toxicity profile, which not showing the effects mutagenicity ($0.94^{(-)}$), immunotoxicity ($0.77^{(-)}$), hepatotoxicity ($0.72^{(-)}$), neurotoxicity ($0.88^{(-)}$), and

Table 1. The Determined Targets, PDB ID, Binding Affinity (kcal/mol), RMSD (Å), and their Interacted Residues with Chrysoeriol and DOX and their Type of Interactions.

S. No.	Targets Name	Targets (UniProt ID)	Binding Affinity (kcal/mol)	RMSD (Å)	Hydrogen Bonds	Hydrophobic Residues	Other Types of Bonds
	Chrysoeriol						
1.	Caspase-3	P42574	−6.7	1.307	HIS121, CYS163, SER205, ARG207(2), PHE250^{CH}, SER251(2)^{CH}	TRP206, PHE252, ASP253	ARG64 (2)^{PC}, TYR204^{PPTS}, PHE256^{PPS}
2.	Caspase-8	Q14790	−6.5	1.709	GLY362, ASP363, TYR365, ARG258^{CH}	ILE257, ASN261, TYR412, PRO415	ARG413^{PC}, ARG260^{A}, HIS317^{PA}, CYS360^{A}, VAL410^{PS}
3.	Caspase-9	P55211	−6.6	2.08	SER307, GLY395	GLU304, ASP305, GLU306, SER310, ASP356, SER359, GLU365, VAL393, LYS394	PRO312^{PA}, TRP362^{UFD}
	DOX						
4.	Caspase-3	P42574	−6.3	2.757	ARG64, ARG207, PHE252, ASP253, SER205^{CH}, SER251^{CH}	HIS121, ASN208, SER209	CYS163^{PA}, TYR204^{PPTS}, PHE256^{PPTS}
5.	Caspase-8	Q14790	−6.3	2.398	ARG258, TYR365, TYR412, HIS317^{CH}	LYS253, SER256, ILE257, ASP259, ARH413, ASN458	ARG258^{A}, LEU254^{A}, ASP363^{PIA}
6.	Caspase-9	P55211	−6.7	2.685	SER310, VAL393, GLY395, LYS394^{CH}, SER307^{CH}	GLU304, GLU306, GLY309, ASN311, PRO312, ASP356, SER359, ASP369, ILE396	LYS394^{PA}, GLU365^{PIA}

Note: CH: Carbon–hydrogen bond; PC: Pi-cation; PPTS: Pi-Pi-T-shaped; PPS: Pi-pi-stacked; A: Alkyl; PA: Pi-alkyl; PS: Pi-sigma; UFD: Unfavorable donor; PIA: Pi-anion.

cytotoxicity ($0.95^{(-)}$) with a predicted LD_{50} value of 4,000 mg/kg, indicating low acute toxicity and can cross BBB mildly. Alternatively, the DOX exhibited a lesser toxicity profile with the lower LD50 value of 205, indicating high acute toxicity, and was classified as BBB class III, suggesting limited brain permeability.

Discussion

Thyroid cancer, recognized as the most frequently diagnosed endocrine malignancy globally, has exhibited a consistent rise in incidence across numerous countries and regions over recent decades. This trend is particularly pronounced among females, with some estimates suggesting a fourfold increase in cases over the past two decades (Bray et al., 2024). This disproportionate effect in females, frequently three to five times higher depending on disease severity, underscores the need for a deeper investigation into sex-specific pathophysiological mechanisms. While enhanced diagnostic capabilities, such as advanced ultrasonography, have undoubtedly contributed to the rising detection rates, particularly for smaller papillary thyroid cancers, intrinsic biological and behavioral factors unique to females may also play a significant role in this epidemiological pattern (Gil-Bernabé et al., 2025). While generally treatable, a significant subset of thyroid cancers, particularly advanced or radioiodine-refractory cases, presents considerable therapeutic challenges. This includes 15%–20% of differentiated thyroid cancer and most anaplastic types, alongside approximately 30% of medullary thyroid cancer cases that exhibit resistance to standard interventions. Despite advances in understanding the disease, uncertainties persist in screening, diagnosis, and treatment approaches for thyroid cancer (Silaghi et al., 2022). For instance, though well-differentiated thyroid cancers typically have favorable prognoses, about 10% of patients experience relapse due to inadequate response to radioactive iodine therapy. This unresponsiveness often stems from the loss of the thyroid cells' ability to uptake radioiodine, a critical mechanism for its therapeutic effect. This resistance necessitates exploration into alternative therapeutic modalities that can circumvent these limitations and provide more effective interventions for patients (Zhang et al., 2018). The results of the present study suggested that chrysoeriol has considerable anti-cancer activity against thyroid cancer cells.

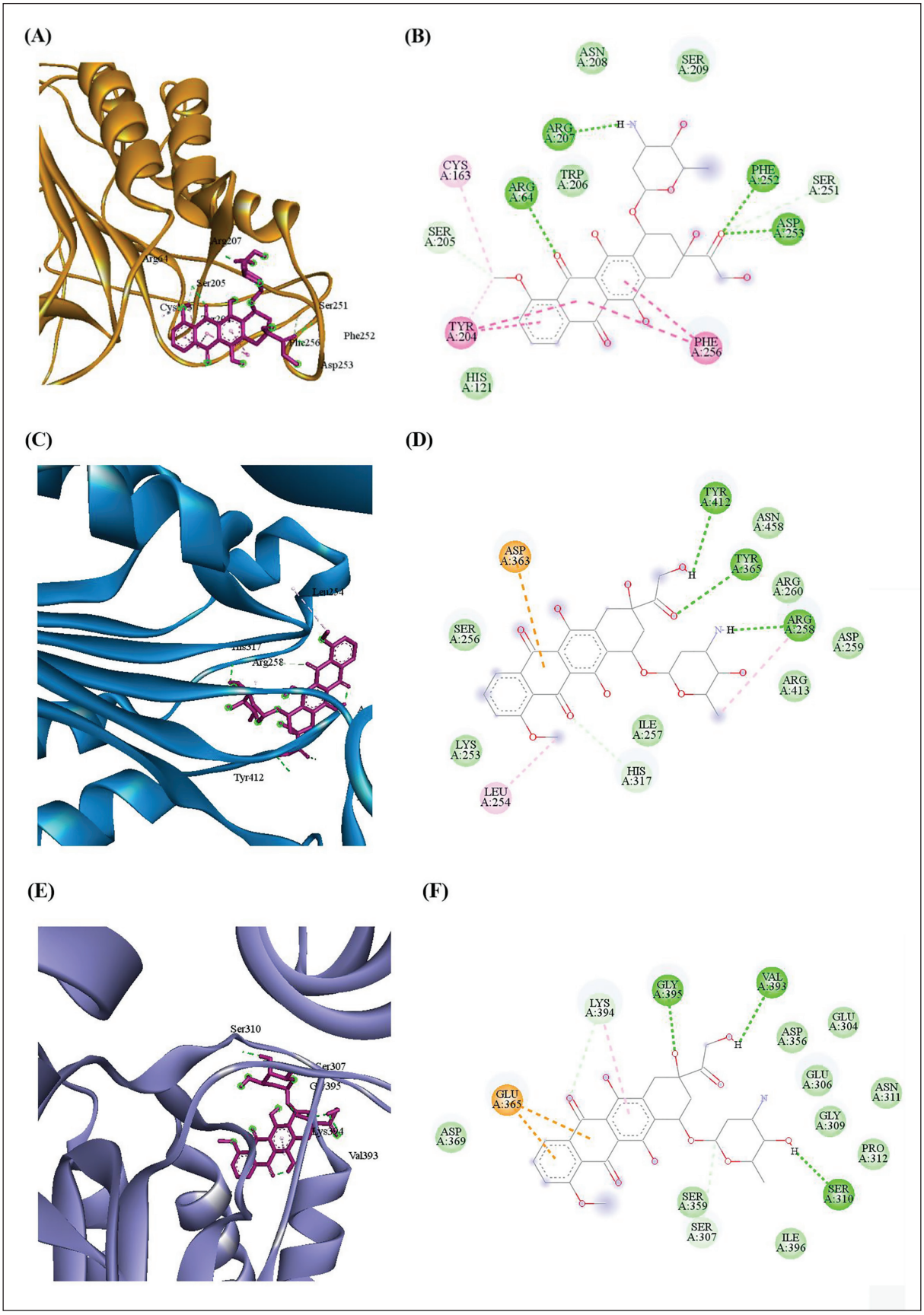


Figure 6. *(continued).*

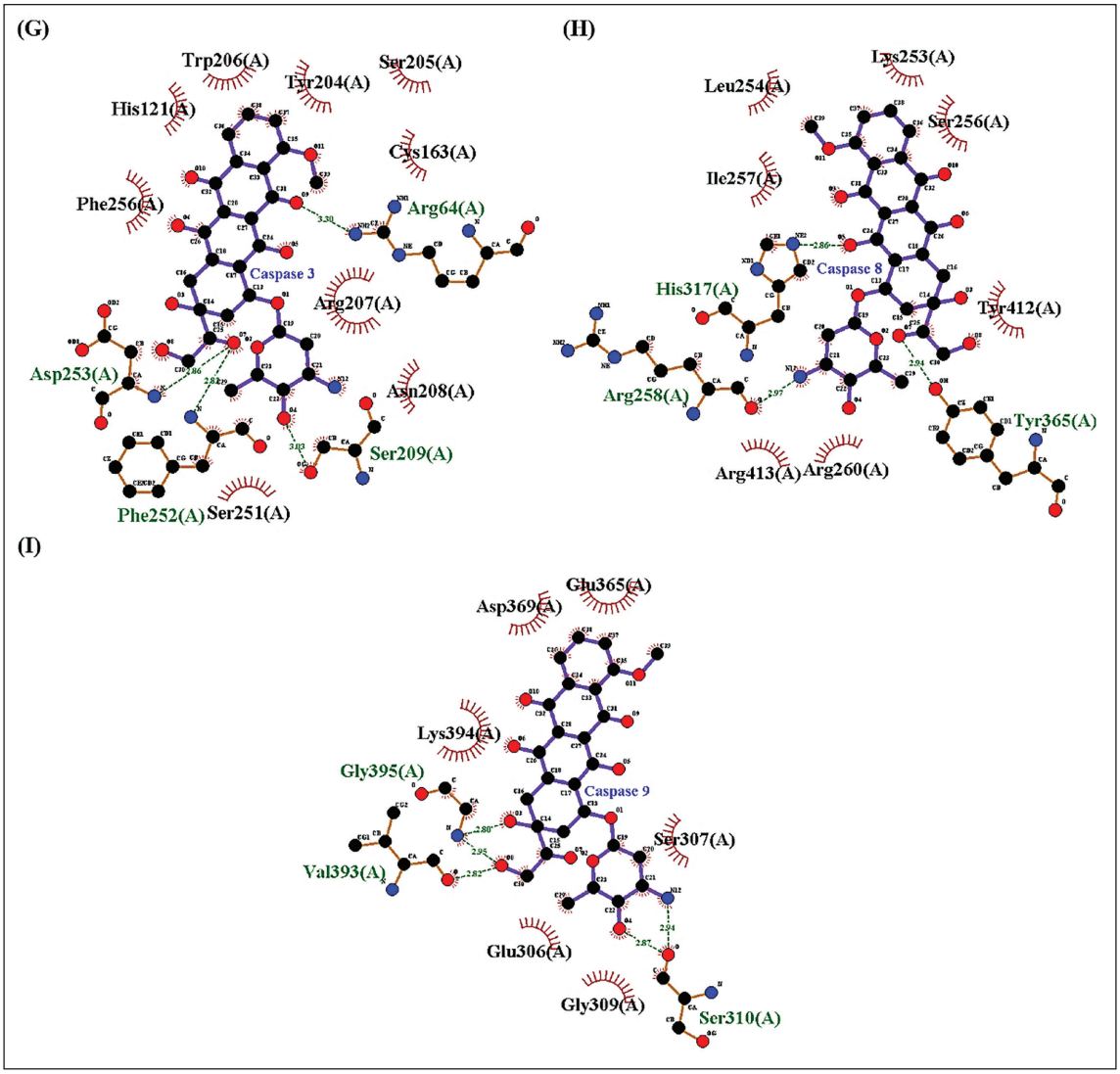


Figure 6. The Three-dimensional (3D) and Two-dimensional (2D) Docking Pose of the Caspase-3, Caspase-8, and Caspase-9 Interacted with the DOX and the LigPlot+ Interactions.

Note: (A, B, G) caspase-3 (C, D, H) caspase-8 (E, F, I) caspase-9.

The evaluation of a drug compound's capacity to induce cellular damage or death in cancer cells is a fundamental step in oncology drug discovery and development. This analysis, termed cytotoxicity testing, provides critical insights into a compound's therapeutic potential and selectivity. It also allows for the differentiation between anti-proliferative effects and direct cell death, which is crucial for elucidating the precise mechanisms of drug action (Zasadil et al., 2014). A key metric in these evaluations is the half-maximal inhibitory concentration, which quantifies the dosage of a compound needed to inhibit 50% of cell viability. Numerous *in vitro* assays are employed to assess cytotoxicity, which evaluate cell viability and proliferation by measuring metabolic activity or cell membrane integrity (Bracci et al., 2014). The MTT assay is a colorimetric method extensively employed for assessing cellular metabolic activity, viability, and cytotoxicity in drug discovery and development, particularly for anti-cancer agents (Gerlier & Thomasset, 1986). This assay quantifies the reduction of the yellow tetrazolium dye MTT into an insoluble purple formazan product by mitochondrial succinate dehydrogenase in metabolically active cells, thereby serving as a reliable indicator of viable cell count and drug efficacy. This method is widely adopted due to its rapidity, convenience, and economic feasibility for quantifying viable cells in culture for both proliferation and cytotoxicity studies (Mello et al., 2020). In the present work, the cytotoxic effect of chrysoeriol against thyroid cancer cells was assessed using the MTT assay. The findings of the MTT assay demonstrated that chrysoeriol treatment substantially inhibited the viability of TPC-1 cells. These findings

Table 2. Toxicity Analysis of the Potential Compound Chrysoeriol and DOX.

S. No.	Compound Name	Toxicity Analysis											
		Mutagenicity	Immunotoxicity	Hepatotoxicity	Neurotoxicity	Respiratory Toxicity	Nephrotoxicity	Cytotoxicity	Carcinogenicity	BBB-Barrier	LD_{50} (mg/kg)	TC
1.	Chrysoeriol	0.94(−)	0.77(−)	0.72(−)	0.88(−)	0.85(+)	0.64(MD)	0.95(−)	0.82(+)	0.52(MD)	4,000	V
2.	DOX	0.98(+)	0.99(+)	0.86(−)	0.74(+)	0.91(+)	0.80(+)	0.94(+)	0.90(−)	1.0(−)	205	III

Note: (−): Negative; (+): Positive; MD: Mild.

demonstrate that chrysoeriol can hinder thyroid cancer cell growth, indicating that it may be an effective cytotoxic agent against thyroid cancer cells.

The evaluation of novel drug compounds for their anticancer efficacy necessitates a meticulous analysis of their capacity to trigger programmed cell death, particularly apoptosis, in tumor cells. This analytical approach is crucial for differentiating between cytotoxic effects that merely halt proliferation and those that actively eliminate malignant cells, thereby elucidating the precise mechanisms of drug action (Schultz & Harrington, 2003). Apoptosis induction is a highly desirable outcome in oncology, as it can lead to sustained tumor regression and potentially prevent drug resistance. Therefore, a comprehensive assessment of apoptotic pathways activated by candidate drugs is indispensable for identifying promising therapeutic agents. Various methodologies are employed to quantify apoptosis, with the dual staining method being a commonly utilized technique to distinguish between live and apoptotic cells (Brunelle & Zhang, 2010). This technique critically distinguishes between viable, early apoptotic, and late apoptotic cells through differential staining based on membrane integrity and chromatin condensation. Live cells exhibit uniform green fluorescence, while early apoptotic cells present yellow fluorescence with bright green dots within the nucleus due to chromatin condensation and nuclear fragmentation (Honda et al., 2000). Conversely, late apoptotic cells show orange to red fluorescence as ethidium bromide binds to fragmented DNA, signifying a loss of membrane integrity. The dual staining method, therefore, serves as a robust qualitative and quantitative tool for assessing apoptotic morphological changes in various cell types, including cancer cells. This method's cost-effectiveness and simplicity make it a widely adopted technique for initial apoptosis detection in cancer cells (Rieger et al., 2010). In this work, the apoptotic activity of chrysoeriol was assessed on the thyroid cancer cells using a dual staining method. The present results revealed that chrysoeriol treatment notably increased the apoptotic cell death in TPC-1 cells. Therefore, it was evident that chrysoeriol can induce apoptosis in thyroid cancer cells, which supports the hypothesis that it can hinder the progression of thyroid cancer.

The caspase pathway, a family of cysteine proteases crucial for cellular homeostasis, predominantly mediates apoptosis. These proteases are broadly classified into initiator and executioner caspases, which operate in a sequential cascade to dismantle cellular components. Initiator caspases, such as caspase-8 and caspase-9, are activated first and subsequently cleave and activate executioner caspases, notably caspase-3, which then orchestrate the systematic degradation of cellular structures (McIlwain et al., 2015). The extrinsic apoptotic cascade is typically commenced by external signals binding to death receptors, resulting in the activation of caspase-8, whereas the intrinsic pathway is triggered by intracellular stressors and involves the activation of caspase-9. The intricate balance between pro- and anti-apoptotic proteins further

regulates the mitochondrial pathway, influencing the ultimate activation of downstream caspases (Tait & Green, 2008).

Understanding these complex interdependencies and the specific roles of caspase-3, caspase-8, and caspase-9 is critical for clarifying the mechanisms of apoptosis and developing targeted therapies for cancer. Specifically, caspase-9 serves as a key indicator for the activation of the intrinsic apoptotic pathway, while caspase-8 signifies the activation of the extrinsic pathway (Kesavardhana et al., 2020). The convergence of these pathways at the level of effector caspases, particularly caspase-3, emphasizes a final common route for programmed cell death, regardless of the initiating stimulus. This intricate interplay underscores how both extrinsic and intrinsic pathways ultimately converge on effector caspases, with caspase-3 playing a central role in the proteolytic cascade that dismantles the cell (Lou et al., 2021). The induction of apoptosis is a critical strategy in oncology, as many cancers exhibit resistance to this natural cellular mechanism. This resistance often stems from oncogenic mutations that disrupt regulatory circuits governing cellular functions, thereby enabling tumor cells to evade pro-apoptotic insults and achieve deregulated proliferation (Constantinou et al., 2009). Consequently, therapeutic interventions aimed at restoring or initiating apoptotic pathways offer a highly effective approach to cancer treatment across various cancer types. Specifically, targeting the caspase cascade offers a promising avenue for developing novel anti-cancer agents (Pozo-Uisado et al., 2005; Seo et al., 2016). Supportively, the current findings indicated that the chrysoeriol treatment markedly increased the caspase-3, caspase-8, and caspase-9 activities in the TPC-1 cells. These results suggest that chrysoeriol treatment can trigger caspase-dependent apoptosis in thyroid cancer cells. Moreover, the molecular docking and toxicity analyses were performed to evaluate the potential interaction mechanisms and safety profile of chrysoeriol, which was compared with the standard chemotherapeutic drug DOX, toward caspase-3, caspase-8, and caspase-9, which play a critical role in the intrinsic and extrinsic apoptotic pathways, which are primarily associated with the induction and execution of programmed cell death.

The docking study revealed that the chrysoeriol exhibited better binding affinities ranging from −6.5 to −6.7 kcal/mol compared to the DOX, and also the low RMSD values (<2.1 Å) described stable and reliable docking conformations. Also, the key catalytic dyad residues HIS121 and CYS163, as well as nearby substrate-recognition residues Ser205 and Arg207, interacted with the chrysoeriol, which could modulate the caspase-3 activation (Bobay et al., 2012; Huang et al., 2021). Also, the residues such as ARG207, SER205, and SER251 act as key active common residues that are involved in the hydrogen or carbon hydrogen bond formation with the chrysoeriol and DOX. These findings indicate that chrysoeriol can potentially enhance caspase activation through direct binding and conformational stabilization, consistent with the observed *in vitro* increase in caspase enzyme activity. Likely, the chrysoeriol interacted with the caspase-8 catalytic triad, which comprises CYS360, HIS317, and ARG258 (Mishra et al., 2023; Watt et al., 1999) and the residues such as ASP363, TYR365, ARG258, ILE257, TYR412, ARG413, and HIS317 involved in the interactions with the chrysoeriol and DOX, respectively. Meanwhile, the residues of caspase-9 which includes SER307, GLY395, GLU304, GLU306, SER310, ASP356, SER359, LYS394, and PRO312 actively involved in the interactions with chrysoeriol and DOX.

Beyond docking, the computational toxicity reveals more aspects regarding the pharmacological safety of the compounds. Chrysoeriol showed a favorable toxicity profile with high LD_{50} (4,000 mg/kg), non-mutagenicity, non-hepatotoxicity, non-carcinogenicity and low BBB permeability. The toxicological data suggest that chrysoeriol could be a safer alternative than traditional chemotherapeutics such as DOX, as it has potent mutagenicity and immunotoxicity, with a low LD_{50} (205 mg/kg), which suggests a high acute toxicity. The strong caspase-binding affinities combined with low predicted toxicity suggest the potential of chrysoeriol to serve as a natural pro-apoptotic modulator, warranting further preclinical studies.

The present study has several limitations that need to be considered in future studies. Firstly, the lack of *in vivo* validation restricts the translation of our findings to clinical settings. Additionally, potential off-target effects of chrysoeriol have not been thoroughly explored, which could impact its safety profile. To address these limitations, our future studies will focus on assessing chrysoeriol's *in vivo* efficacy using xenograft models, providing a more comprehensive understanding of its therapeutic potential. We also plan to explore combinatorial approaches with existing therapies, such as doxorubicin or kinase inhibitors, to enhance therapeutic outcomes and minimize potential resistance mechanisms. These studies will be crucial in advancing chrysoeriol's clinical translation and evaluating its potential as a viable anti-cancer agent. By addressing these limitations, we aim to provide a more robust foundation for chrysoeriol's therapeutic application.

Conclusion

The present study shows that chrysoeriol exhibits anti-cancer properties against thyroid cancer, diminishing cell growth and triggering apoptosis in TPC-1 cells through the upregulation of caspase activity. The treatment with chrysoeriol markedly inhibited cell proliferation and triggered caspase-dependent cell death in TPC-1 cells. Also, the computational analysis confirmed that the chrysoeriol could interact with the catalytic dyad (HIS121 and CYS163) and triad (CYS360, HIS317, and ARG258) of caspase-3 and caspase-8. Additionally, the toxicity analysis described that the chrysoeriol exhibited a safer toxicity profile than the standard drug DOX. Altogether, the current results highlight that

chrysoeriol is a hopeful anti-cancer drug for future thyroid cancer treatment. Furthermore, future investigations are highly recommended to comprehensively elucidate the precise anti-cancer functions of chrysoeriol on thyroid cancer.

Abbreviations

A: Alkyl; AO/EB: Acridine orange/ethidium bromide; CH: Carbon–hydrogen bond; MD: Mild; MTT: 3-(4,5-Dimethylthiazol-2-yl)-2,5-diphenyltetrazolium bromide; PA: Pi-alkyl; PC: Pi-cation; PIA: Pi-anion; PPTS: Pi-Pi-T-shaped; PPS: Pi-pi-stacked; PS: Pi-sigma; TC: Toxicity class; UFD: Unfavorable donor.

Declaration of Conflicting Interests

The authors declared no potential conflicts of interest with respect to the research, authorship, and/or publication of this article.

Ethical Approval

The experiment was approved by the animal committee of the Affiliated Hospital of Hebei University.

Funding

The authors received no financial support for the research, authorship, and/or publication of this article.

ORCID iD

Na Feng https://orcid.org/0009-0000-3564-2941

References

Banerjee, P., Kemmler, E., Dunkel, M., & Preissner, R. (2024). ProTox 3.0: A webserver for the prediction of toxicity of chemicals. *Nucleic Acids Research*, *52*(W1), W513–W520.

Bobay, B. G., Stewart, A. L., Tucker, A.T., Thompson, R. J., Varney, K. M., & Cavanagh, J. (2012). Structural insights into the calcium-dependent interaction between calbindin-D28K and caspase-3. *FEBS Letters*, *586*(20), 3582–3589.

Bracci, L., Schiavoni, G., Sistigu, A., & Belardelli, F. (2014). Immune-based mechanisms of cytotoxic chemotherapy: Implications for the design of novel and rationale-based combined treatments against cancer. *Cell Death & Differentiation*, *21*, 15–25.

Bray, F., Laversanne, M., Sung, H., Ferlay, J., Siegel, R. L., Soerjomataram, I., & Jemal, A. (2024). Global Cancer Statistics 2022: GLOBOCAN estimates of incidence and mortality worldwide for 36 cancers in 185 countries. *CA: A Cancer Journal for Clinicians*, *74*(3), 229–263.

Brunelle, J. K., & Zhang, B. (2010). Apoptosis assays for quantifying the bioactivity of anticancer drug products. *Drug Resistance Updates*, *13*(6), 172–179.

Busaidy, N. L., Konda, B., Wei, L., Wirth, L. J., Devine, C., Daniels, G. A., DeSouza, J. A., Poi, M., Seligson, N. D., Cabanillas, M. E., Sipos, J. A., Ringel, M. D., Eisfeld, A. K., Timmers, C., & Shah, M. H. (2022). Dabrafenib versus dabrafenib + trametinib in *BRAF*-mutated radioactive iodine refractory differentiated thyroid cancer: Results of a randomized, phase 2, open-label multicenter trial. *Thyroid*, *32*(10), 1184–1192.

Christofer Juhlin, C., Mete, O., & Baloch, Z. W. (2023). The 2022 WHO classification of thyroid tumors: Novel concepts in nomenclature and grading. *Endocrine-Related Cancer*, *30*, e220293.

Constantinou, C., Papas, K. A., & Constantinou, A. I. (2009). Caspase-independent pathways of programmed cell death: The unraveling of new targets of cancer therapy? *Current Cancer Drug Targets*, *9*, 717–728.

Dierks, C., Seufert, J., Aumann, K., Ruf, J., Klein, C., Kiefer, S., Rassner, M., Boerries, M., Zielke, A., la Rosee, P., Meyer, P. T., Kroiss, M., Weißenberger, C., Schumacher, T., Metzger, P., Weiss, H., Smaxwil, C., Laubner, K., Duyster, J., von Bubnoff, N., Miething, C., & Thomusch, O. (2021). Combination of lenvatinib and pembrolizumab is an effective treatment option for anaplastic and poorly differentiated thyroid carcinoma. *Thyroid*, *31*(7), 1076–1085.

Eberhardt, J., Santos-Martins, D., Tillack, A. F., & Forli, S. (2021). AutoDock Vina 1.2.0: New docking methods, expanded force field, and python bindings. *Journal of Chemical Information and Modeling*, *61*(8), 3891–3898.

French, J. D., Haugen, B. R., Worden, F. P., Bowles, D. W., Gianoukakis, A. G., Konda, B., Dadu, R., Sherman, E. J., McCue, S., Foster, N. R., Nikiforov, Y. E., Farias, T. D. J., Norman, P. J., & Wirth, L. J. (2024). Combination targeted therapy with pembrolizumab and lenvatinib in progressive, radioiodine-refractory differentiated thyroid cancers. *Clinical Cancer Research*, *30*(17), 3757–3767.

Gerlier, D., & Thomasset, N. (1986). Use of MTT colorimetric assay to measure cell activation. *Journal of Immunological Methods*, *94*(1), 57–63.

Gil-Bernabé, S., García-DeLaFuente, L., & García-Rostán, G. (2025). The revolution of targeted therapies in thyroid cancer treatment: Present and future promising anti-cancer drugs. *International Journal of Molecular Sciences*, *26*(8), 3663.

Heo, L., Park, H., & Seok, C. (2013). GalaxyRefine: Protein structure refinement driven by side-chain repacking. *Nucleic Acids Research*, *41*(W1), W384–W388.

Honda, O., Kuroda, M., Joja, I., Asaumi, J., Takeda, Y., Akaki, S., Togami, I., Kanazawa, S., Kawasaki, S., & Hiraki, Y. (2000). Assessment of secondary necrosis of Jurkat cells using a new microscopic system and double staining method with annexin V and propidium iodide. *International Journal of Oncology*, *16*(2), 283–288.

Huang, S., Mei, H., Lu, L., Kuang, Z., Heng, Y., Xu, L., Liang, X., Qiu, M., & Pan, X. (2021). Conformational transitions of caspase-6 in substrate-induced activation process explored by perturbation-response scanning combined with targeted molecular dynamics. *Computational and Structural Biotechnology Journal*, *19*, 4156–4164.

Jendele, L., Krivak, R., Skoda, P., Novotny, M., & Hoksza, D. (2019). PrankWeb: A web server for ligand binding site prediction and visualization. *Nucleic Acids Research*, *47*(W1), W345–W349.

Kaczmarzyk, I., Nowak-Perlak, M., & Woźniak, M. (2024). Promising approaches in plant-based therapies for thyroid cancer: An overview of *in vitro, in vivo*, and clinical trial studies. *International Journal of Molecular Sciences*, *25*(8), 4463.

Kesavardhana, S., Malireddi, R. K. S., & Kanneganti, T. D. (2020). Caspases in cell death, inflammation, and pyroptosis. *Annual Review of Immunology*, *38*, 567–595.

Kim, M. H., Kwon, S. Y., Woo, S. Y., Seo, W. D., & Kim, D. Y. (2021). Antioxidative effects of chrysoeriol via activation of the Nrf2 signaling pathway and modulation of mitochondrial function. *Molecules*, *26*(2), 313.

Kitahara, C. M., & Schneider, A. B. (2022). Epidemiology of thyroid cancer. *Cancer Epidemiology, Biomarkers & Prevention*, *31*, 1284–1297.

Lamartina, L., Leboulleux, S., & Schlumberger, M. (2021). Thyroid cancer incidence in children and adolescents. *Lancet Diabetes & Endocrinology*, *9*, 128–129.

Laskowski, R. A., & Swindells, M. B. (2011). LigPlot+: Multiple ligand–protein interaction diagrams for drug discovery. *Journal of Chemical Information and Modeling*, *51*(10), 2778–2786.

Liu, Z., Song, X., Xin, Y., Wang, X., Yu, H., Bai, Y., Liu, J., Zhang, C., & Hui, R. (2009). Protective effect of chrysoeriol against doxorubicin-induced cardiotoxicity *in vitro*. *Chinese Medical Journal*, *122*, 2652–2656.

Liu, Y. X., Chen, Y. J., Xu, B. W., Fu, X. Q., Ding, W. J., Li, S. A., Wang, X. Q., Wu, J. Y., Wu, Y., Dou, X., Liu, B., & Yu, Z. L. (2023). Inhibition of STAT3 signaling contributes to the anti-melanoma effects of chrysoeriol. *Phytomedicine*, *109*, 154572.

Lou, J., Zhou, Y., Feng, Z., Ma, M., Yao, Y., Wang, Y., Deng, Y., & Wu, Y. (2021). Caspase-independent regulated necrosis pathways as potential targets in cancer management. *Frontiers in Oncology*, *10*, 616952.

McIlwain, D. R., Berger, T., & Mak, T. W. (2015). Caspase functions in cell death and disease. *Cold Spring Harbor Perspectives in Biology*, *7*, a026716.

Mello, D. F., Trevisan, R., Rivera, N., Geitner, N. K., Di Giulio, R. T., Wiesner, M. R., Hsu-Kim, H., & Meyer, J. N. (2020). Caveats to the use of MTT, neutral red, Hoechst and Resazurin to measure silver nanoparticle cytotoxicity. *Chemico-Biological Interactions*, *315*, 108868.

Min, D. Y., Jung, E., Ahn, S. S., Lee, Y. H., Lim, Y., & Shin, S. Y. (2020). Chrysoeriol prevents TNFα-induced CYP19 gene expression via EGR-1 downregulation in MCF7 breast cancer cells. *International Journal of Molecular Sciences*, *21*(20), 7523.

Mishra, D., Mishra, A., Rai, S. N., Singh, S. K., Vamanu, E., & Singh, M. P. (2023). *In silico* insight to identify potential inhibitors of BUB1B from mushroom bioactive compounds to prevent breast cancer metastasis. *Frontiers in Bioscience*, *28*(7), 151.

Pizzato, M., Li, M., Vignat, J., Laversanne, M., Singh, D., La Vecchia, C., & Vaccarella, S. (2022). The epidemiological landscape of thyroid cancer worldwide: GLOBOCAN estimates for incidence and mortality rates in 2020. *Lancet Diabetes & Endocrinology*, *10*(4), 264–272.

Pozo-Uisado, E., Merino, J. M., Mulero-Navarro, S., Lorenzo-Benayas, M. J., Centeno, F., Alvarez-Barrientos, A., & Fernandez Salguero, P. M. (2005). Resveratrol-induced apoptosis in MCF-7 human breast cancer cells involves a caspase-independent mechanism with downregulation of Bcl-2 and NF-kappa B. *International Journal of Cancer*, *116*, 1004.

Qiu, C., & Xu, Y. (2021). Chrysoeriol attenuates cisplatin induced acute kidney injury in a rat model by regulating PI3K/AKT and NF-[kappa]B pathways. *Current Topics in Nutraceutical Research*, *19*, 366–373.

Rieger, A. M., Hall, B. E., Luong, L. T., Schang, L. M., & Barreda, D. R. (2010). Conventional apoptosis assays using propidium iodide generate a significant number of false positives that prevent accurate assessment of cell death. *Journal of Immunological Methods*, *358*(1), 81–92.

Schultz, D. R., & Harrington, W. J. (2003). Apoptosis: Programmed cell death at a molecular level. *Seminars in Arthritis and Rheumatism*, *32*(6), 345–369.

Seo, H. S., Ku, J. M., Choi, H. S., Choi, Y. K., Woo, J. K., Kim, M., Kim, I., Na, C. H., Hur, H., Jang, B. H., Shin, Y. C., & Ko, S. G. (2016). Quercetin induces caspase-dependent extrinsic apoptosis through inhibition of signal transducer and activator of transcription 3 signaling in HER2-overexpressing BT-474 breast cancer cells. *Oncology Reports*, *36*(1), 31–42.

Siegel, R. L., Miller, K. D., Wagle, N. S., & Jemal, A. (2023). Cancer statistics, 2023. *CA: A Cancer Journal for Clinicians*, *73*, 17–48.

Silaghi, H., Lozovanu, V., Georgescu, C. E., Pop, C., Nasui, B. A., Cătoi, A. F., & Silaghi, C. A. (2022). State of the art in the current management and future directions of targeted therapy for differentiated thyroid cancer. *International Journal of Molecular Sciences*, *23*(7), 3470.

Tait, S. W. G., & Green, D. R. (2008). Caspase-independent cell death: Leaving the set without the final cut. *Oncogene*, *27*, 6452–6461.

Thumpati, P., Rai, S. N., Prajapati, C., Ramakrishna, K., & Singh, S. K. (2025). Targeting c-MYC G-quadruplexes for cancer treatment with small molecules. *Scientia Pharmaceutica*, *93*, 6.

Varadi, M., Bertoni, D., Magana, P., Paramval, U., Pidruchna, I., Radhakrishnan, M., Tsenkov, M., Nair, S., Mirdita, M., Yeo, J., Kovalevskiy, O., Tunyasuvunakool, K., Laydon, A., Žídek, A., Tomlinson, H., Hariharan, D., Abrahamson, J., Green, T., Jumper, J., & Velankar, S. (2024). AlphaFold protein structure database in 2024: Providing structure coverage for over 214 million protein sequences. *Nucleic Acids Research*, *52*(D1), D368–D375.

Watt, W., Koeplinger, K. A., Mildner, A. M., Heinrikson, R. L., Tomasselli, A. G., & Watenpaugh, K. D. (1999). The atomic-resolution structure of human caspase-8, a key activator of apoptosis. *Structure*, *7*(9), 1135–1143.

Wei, W., He, J., Ruan, H., & Wang, Y. (2019). *In vitro* and *in vivo* cytotoxic effects of chrysoeriol in human lung carcinoma are facilitated through activation of autophagy, sub-G1/G0 cell cycle arrest, cell migration and invasion inhibition and modulation of MAPK/ERK signalling pathway. *Journal of BUON*, *24*, 936–942.

Wongkularb, S., Limboonreung, T., Tuchinda, P., & Chongthammakun, S. (2022). Suppression of PI3K/Akt/MTOR pathway in chrysoeriol-induced apoptosis of rat C6 glioma cells. *In Vitro Cellular & Developmental Biology—Animal*, *58*, 29–36.

Wu, J. Y., Chen, Y. J., Bai, L., Liu, Y. X., Fu, X. Q., Zhu, P. L., Li, J. K., Chou, J. Y., Yin, C. L., Wang, Y. P., Bai, J. X., Wu, Y., Wu, Z. Z., & Yu, Z. L. (2020). Chrysoeriol ameliorates TPA-induced acute skin inflammation in mice and inhibits NF-κB and STAT3 pathways. *Phytomedicine*, *68*, 153173.

Zasadil, L. M., Andersen, K. A., Yeum, D., Rocque, G. B., Wilke, L. G., Tevaarwerk, A. J., Raines, R. T., Burkard, M. E., & Weaver, B. A. (2014). Cytotoxicity of paclitaxel in breast cancer is due to chromosome missegregation on multipolar spindles. *Science Translational Medicine*, *6*(229), 229ra43.

Zhang, Y., Li, Z., Min, Q., Palida, A., Zhang, Y., Tang, R., Chen, L., & Li, H. (2018). 8-Chrysoeriol, as a potential BCL-2 inhibitor triggers apoptosis of SW1990 pancreatic cancer cells. *Bioorganic Chemistry*, *77*, 478–484.

Zhao, Y., Zhao, S., Fan, Z., Zhao, Y., & Wang, G. (2025). Relationship between programmed cell death and targeted therapy for thyroid cancer in patients with a poor prognosis: An update. *Discover Oncology*, *16*(1), 112.